22

Structure of Weak shock waves in bubbly liquid

by

Ryuji Ishii* and Takeshi Hashimoto**

* Department of Aeronautical Engineering, Kyoto University

** Toyota Motor Cooporation, Toyota 471

ABSTRACT

In this paper, steady and unsteady weak shock waves in a bubbly liquid are treated numerically. A new system of model equations describing the bubbly flow is applied and the flow structure behind a shock front is investigated in detail. It is shown that the heat conduction between the liquid and the gas phases through the bubble surface affects significantly the wave profile near the shock front. It is, however, shown that the velocity difference between the liquid and the gas phases affects the wave profile remarkably for weak shock waves. Radial oscillation of bubbles tends to produce oscillatory profile of the mixture pressure especially near the wave fronts. Numerical simulation shows that the weak shock consists of a precursor near the shock front and a main shock downstream of it. It is confirmed that the stationary shock wave for a constant polytropic-exponent model is realized as an asymptotic solution for a shock tube problem with uniform conditions in the low pressure and high pressure chambers.

I. INTRODUCTION

So far, the problem of propagation of shock waves through a bubbly liquid has received considerable attention. The speed of shock wave propagating through a liquid containing small gas bubbles was first studied theoretically and experimentally by Campbell and Pitcher[1]. Later, Crespo[2] investigated analytically the shock structure under some simplifying assumptions Noordzij & Wijngaarden[3] performed experiments of shock propagation in a bubbly liquid and found that there are three types of shock structure.

Recently, Beylich & Gülhan[4] performed systematic numerical simulation and experiment of shock waves in bubbly liquid and obtained good agreement between them. In their analysis, however, a few empirical parameters are introduced to fit the numerical results to the experiments.

In many previous papers,the effects of velocity difference between the two-phases on the shock waves are assumed to be negligible. This assmption is not always appropriate for the weak shock wave. Although in general the thermal dissipation plays the most important role in the determination of the shock structure, the effect of the relative translational motion of the bubbles can not be neglected, especially for weak shock waves. Dispersion and dissipation processes associated with the expanding and contracting motions of bubbles usually affect the shock structure rather in the region near the shock front. The shock structure, however, cannot be predicted precisely without considering the effect of the velocity difference between the two phases as well as that of the thermal dissipation.

In the present paper, first stationary shock waves in a bubbly liquid are treated. Here the weak shock wave is defined as the shock with a pressure ratio less than or at most equal to the ratio of specific heats of the gas γ. The detailed flow structure behind the shock front and the effect of the velocity difference between the two-phases on the shock structure is investigated numerically. Next shock tube problems are treated and unsteady behavior of the shocks is discussed. All the numerical simulations are performed on a supercomputer Fujitsu VP-2600 in the Data Processing Center of Kyoto University.

II. BASIC EQUATIONS

We consider a one-dimensional flow of a mixture composed of an incompressible liquid and small gas bubbles dispersed in it. It is assumed that the bubbles remain spherical throughout the flow, have locally uniform size and do not break up or coalesce, the pressure within each bubble is uniform, no phase change takes place and the temperature of the liquid remains constant throughout the flow.

Under these assumptions, the governing equations for a one-dimensional unsteady flow are given as[5]

$$\frac{\partial}{\partial t}(1-\alpha)+\frac{\partial}{\partial x}[(1-\alpha)u_\ell] = 0, \tag{1}$$

$$\frac{\partial}{\partial t}(\rho_g\alpha) + \frac{\partial}{\partial x}(\rho_g\alpha u_g) = 0, \tag{2}$$

$$\frac{\partial}{\partial t}[(1-\alpha)u_\ell]+\frac{\partial}{\partial x}[(1-\alpha)u_\ell^2+p] = 0, \tag{3}$$

$$\frac{D_g u}{Dt} + \frac{\varepsilon}{k\tau}\frac{D_g}{Dt}(k\tau)-(1+\frac{1}{k})\frac{D_\ell u_\ell}{Dt} + \frac{D_M}{k\alpha}\frac{\partial}{\partial x}(\alpha\rho_g)$$

$$+ \frac{H}{k\alpha}\frac{\partial}{\partial x}(\frac{D_g\alpha}{Dt}) = -\frac{9}{Re}\frac{\varepsilon}{kR^2}, \tag{4}$$

where

$$\tau = \frac{1}{\rho_g} = R^3, \tag{5}$$

$$\varepsilon = u_g-u_\ell, \tag{6}$$

$$k = \frac{1}{2}(1+\lambda\alpha), \tag{7}$$

$$\frac{D_g}{Dt} = \frac{\partial}{\partial t} +u_g\frac{\partial}{\partial x}, \quad \frac{D_\ell}{Dt} = \frac{\partial}{\partial t} +u_\ell\frac{\partial}{\partial x}. \tag{8}$$

Here the time t, the space coordinate x, the fluid velocity u, the pressure p, the gas density ρ_g, the bubble radius R, and the coefficients of diffusion force and replusive force, D_M and H, are nondimensionalized by R_0/U_0, R_0, U_0, $\rho_\ell U_0^2$, ρ_{g0}, R_0, $(4/3)\pi R_0^3\rho_\ell U_0^2$, R_0U_0, respectively, where U_0 is a reference velocity. The subscript zero denotes the uniform flow conditions ahead of the shock front and the subscripts g and ℓ denote the gas phase and the liquid phase, respectively. The parameter λ in the added mass coefficient of a spherical bubble k in Eq.(7) is given by Wijngaarden[6] as λ =2.78. The bubble Reynolds number in Eq. (4) is defined by

$$Re = \frac{\rho_\ell U_0 R_0}{\mu_\ell}. \tag{9}$$

The parameters D_M and H first introduced by Batchelor[7] are quantities that can be determined at least in principle from the detailed study of hydrodynamic interactions between bubbles. Unfortunately, these forces have not yet been evaluated theoretically. In the following analysis, therefore, D_M and H are assumed to be small positive constants.

Since the gas inside each bubble is compressible, two more equations are needed to close the system. These are the momentum equation for radial motion of each bubble and the equation of state of the gas inside the bubble. The first is given in the nondimensional form as

$$p_g-p = R\frac{D_g^2R}{Dt^2} + \frac{3}{2}(\frac{D_gR}{Dt})^2 + \frac{4\Psi}{Re}\frac{1}{R}\frac{D_gR}{Dt}, \tag{10}$$

which is the so called Rayleigh-Plesset equation where the parameter Ψ is a correction factor due to dissipation processes in the liquid phases. The damping factor Ψ in Eq.(10) is approximated to be a constant given by the linear analysis of Devin[9].

The second is given by

$$p_g = \Gamma\rho_g^n \tag{11}$$

where n is an effective polytropic exponent of the gas. The nondimensional parameter Γ is defined by

$$\Gamma = \frac{p_0}{\rho_\ell U_0^2}. \tag{12}$$

In the analysis of the bubbly liquid, sometimes the polytropic exponent n is assumed to be some constant in the range from 1 to γ. In such a case, the effect of the thermal dissipation can be included in the parameter Ψ in Eq.(10)[8].

Strictly speaking, the gas temperature and the density inside the bubble is not uniform even under the reasonable assumption of uniform gas pressure.[9] But to make the problem tractable numerically or analytically, some averaging of the gas density over each bubble is inevitable. This averaging process is closely connected to evaluation of the thermal damping or the polytropic exponent n.

In the present paper, only weak shock waves are considered and then the temperature field is solved by a linear approximation to evaluate the value of n. Although the shock phenomenon is nonlinear and then the main system of Eqs.(1) to (4) must be solved directly as a nonlinear system, only the temperature field is solved by a linear analysis.

By putting

$$p_g = 1+p_g', \quad \rho_g = 1+\rho_g', \tag{13}$$

it is given from Eq.(14) that

$$p_g' = \Gamma n\rho_g', \quad \text{or} \quad n = \frac{p_g'}{\Gamma\rho_g'}. \tag{14}$$

Under the simplifying approximation of uniform pressure in the bubble and the constant temperature of the liquid at the bubble surface, we get

$$\Gamma\rho_g'(t)= \frac{1}{\gamma}p_g'(t)$$

$$+6(1-\frac{1}{\gamma})\frac{D}{\Gamma}\sum_j\int_0^t p_g'(s)\exp[-\frac{D}{\Gamma}\pi^2j^2(t-s)]ds, \tag{15a}$$

$$\text{along} \quad \frac{dx_g}{dt} = u_g, \tag{15b}$$

where

$$D = \frac{\chi_g}{R_0U_0}, \quad \chi_g = \frac{\kappa_{g0}}{\rho_{g0}C_{pg}}. \tag{16}$$

Here κ_g and χ_g are the thermal conductivity and diffusivity of the gas, respectively and C_{pg} is the specific heat at constant pressure. The gas density ρ_g' in Eq.(15a) is defined as an averaged density over the bubble.

It is reasonably expected that the gas phase will behave nearly adiabatically near the shock front ($n\sim\gamma$) but nearly isothermally far downstream ($n\sim1$). But this is not always the case and should be modified. Here it has to be pointed out that the polytropic exponent n can take, at least theoretically, any value from $-\infty$ to $+\infty$. This is very important in the discussion of shock structure.

III. STATIONARY SHOCK WAVES

A. Numerical scheme

For stationary shock waves, the coordinate system (t,x) is transformed into (ξ, η) by

$$\xi = x + U_s t, \quad \eta = t \tag{17}$$

where U_s is the speed of shock wave defined later. After straightforward but lengthy manipulation, Eqs.(1) to (4) and (10) in conjunction with Eqs.(5) to (7) are rearranged by making use of the relation $\partial()/\partial\eta = 0$ to yield

$$\frac{d\beta}{d\xi} + \frac{\beta}{\rho_g}\frac{d\rho_g}{d\xi} - \frac{\varepsilon}{U_s}\beta^2\rho_g\left(\frac{\lambda\alpha_0}{1+\lambda\alpha_0\beta}\frac{d\beta}{d\xi} - \frac{1}{\rho_g}\frac{d\rho_g}{d\xi}\right)$$
$$+\alpha_0\left(1+\frac{1}{k}\right)\beta^3\rho_g{}^2\frac{(1-\alpha_0)^2}{(1-\alpha_0\beta)^3}\frac{d\beta}{d\xi}$$
$$-\frac{9}{Re k U_s}\beta^2\rho_g{}^{11/3}\frac{\varepsilon}{U_s} = 0, \tag{18}$$

$$\frac{d^2\rho_g}{d\xi^2} - \frac{17}{6}\frac{1}{\rho_g}\left(\frac{d\rho_g}{d\xi}\right)^2 - \frac{1}{\beta}\frac{d\beta}{d\xi}\frac{d\rho_g}{d\xi}$$
$$+\left(\frac{4\Psi}{Re U_s}\right)\beta\rho_g{}^{5/3}\frac{d\rho_g}{d\xi} + \frac{3\Gamma}{U_s{}^2}\beta^2\rho_g{}^{11/3}\frac{\Delta p}{\Gamma} = 0, \tag{19}$$

where

$$\beta = \frac{\alpha}{\alpha_0}, \quad \frac{\varepsilon}{U_s} = \frac{1-\beta}{\beta}\frac{\rho_g}{\rho_g} + \alpha_0\frac{1-\beta}{1-\alpha_0\beta}, \tag{20}$$
$$\frac{\Delta p}{\Gamma} = \rho_g{}^n - 1 + \frac{\rho_{g1}(1-\rho_{g1})(\beta-1)}{(1-\rho_{g1})(1-\alpha_0\beta)}, \quad U_s{}^2 = \frac{\Gamma\rho_{g1}}{\alpha_0(1-\alpha_0)}.$$

The above system is subject to the boundary conditions

$$u_g = u_t = 0, \ \rho_g = 1, \ \alpha = \alpha_0, \ p = p_g = \Gamma, \ n_0 = \gamma,$$
at $x = -\infty$, and
$$u_g = u_t, \ \rho_g = \rho_{g1}, \ \alpha = \alpha_1, \ p = p_g = \Gamma\rho_{g1}, \ n_1 = 1, \tag{21}$$
at $x = \infty$.

Numerically the shock front is approximately located at $x = 0$. The subscript 1 denotes flow conditions far downstream of the shock. In thes equations, the diffusion and the repulsive force are neglected. This is because the steady solution is free from ill-posedness of the system a an initial value problem and moreover these forces do not affect appreciably the flow properties[5].

Since Eqs. (18) and (19) in conjunction with Eqs.(15) and (20) constitute a system of simultaneous ordinary differential equations for β and ρ_g, they can be solved for the boundary conditions (21).

The numerical simulations are performed for bubbly liquids composed of air and water. The reference velocity U_0 is put to 10 m/s so as to make the parameter Γ order unity for analytical numerical convenience.

The fourth-order Runge-Kutta-Gill method was adopted for the numerical simulation of stationary shock waves. Undisturbed flow conditions are $p_0 = 1.013\times10^5$ N/m², $T_0 = 15$ °C, $\alpha_0 = 0.05$, and $R_0 = 0.5$mm.

B. Shock front

Before proceeding to the numerical discussions, here the wave profile near the shock front is investigated in detail.

Eqs.(18) and (19) are combined to yield in conjunction with (10) and (15)

$$C_0\frac{d^3\rho_g'}{d\xi^3} + C_1\frac{d^2\rho_g'}{d\xi^2} + C_2\frac{d\rho_g'}{d\xi} + C_3\rho_g' = 0, \tag{22}$$

near the shock front, where

$$C_0 = 1+\alpha_0\left(1+\frac{1}{k_0}\right),$$
$$C_1 = \left[1+\alpha_0\left(1+\frac{1}{k_0}\right)\right]\frac{4\Psi}{Re U_s} + \frac{9}{(1-\alpha_0)Re k_0 U_s},$$
$$C_2 = \frac{3\Gamma}{U_s{}^2}\left\{n_0\left[1+\alpha_0\left(1+\frac{1}{k_0}\right)\right] - \frac{\theta}{(1-\alpha_0)}\right\}$$
$$+\frac{36\Psi}{(1-\alpha_0)(Re U_s)^2 k_0}, \tag{23}$$
$$C_3 = \frac{27\Gamma(n_0-\theta)}{(1-\alpha_0)Re k_0 U_s{}^3}.$$

Here n_0 is the polytropic exponent at the shock front and $\theta = p_1/p_0$. Since $D\xi/U_s \ll 1$ near the shock front, n_0 should be taken as γ.

If we assume a solution to Eq.(22) in the form $\rho_g' = \exp(\lambda\xi)$, we can get

$$\lambda_1 = a+ib, \ \lambda_2 = a-ib, \ \lambda_3 = c, \ \text{for } 1<\theta<n_c$$
$$\lambda_1 = a, \ \lambda_2 = b, \ \lambda_3 = c, \ \text{for } \theta \gtrless n_c, \tag{24}$$

where a, b, c and n_c are real constants. For the pressure ratio θ less than or equal to $n_0(=\gamma)$, both a and c are negative and b is not zero, which means the shock front is a stable spiral

point in the phase plane. For $\gamma < n_0 < n_c$, we have $a<0$, $c>0$, and $b \neq 0$, and then the shock front is an unstable spiral point, where n_c is a constant greater than γ depending on $p_1/p_0, \alpha_0$, Re and Ψ. For $n_0 > n_c$, we have $a<0$, $c>0$, and $b<0$, which means that the shock front is an unstable saddle point.

Summarizing the above results, it can be said that the stationary shock can exit only for $\theta > \gamma$. The shock front is oscillatory for $\gamma < \theta < n_c$ and non-oscillatory for $n_c < \theta$. In Fig.1, a sample of the numerical results for n_c is shown.

From the entropy consideration, however, the stationary shock can exist for $1 < \theta$ as shown by Campbell and Pitcher[1]. Experiments have also shown the possibility of presence of the stationary shock even for $0 < 1 < \theta$[2]. Numerical results in the present analysis actually show the presence of stationary shocks even for $1 < \theta < \gamma$.

When some disturbance is added to the shock front, however small it is, the oscillatory motion is initiated following the solution to Eq.(22). Then the polytropic exponent n changes from γ drastically and can take any value less than θ at least temporarily. When n becomes less than θ, the shock front shifts from a stable spiral point to an unstable saddle or spiral point and then the solution curve will tend to proceed toward another stable point, the downstream end of the shock.

The structure of the weak shock is, therefore, divided into two parts. The front part is essentially oscillatory and its shape depends on the initial disturbances introduced at the shock front. Here we will name this part "precursor". The latter part is essentially stable and it does not depend on the small initial disturbances introduced artificially at the shock front. We call this "main shock" here.

Theoretically Eq.(11) defining the polytropic exponent n is responsible for the precursor. As was shown previously, the polytropic exponent n can take any value from $-\infty$ to $+\infty$ when the oscillatory pressure fluctuation is imposed on the bubble, however small the fluctuation is. Then the polytropic exponent n_0 at the shock front cannot always be specified as $n_0 = \gamma$. In light of this, it will be reasonable to consider that the approximation with a constant exponent n ($\leqq p_1/p_0$) can be one of the possible approximations at least for the analysis of the weak shock wave[3]. Here we call this "constant exponent model".

C. Numerical results

In Fig.2, pressure profiles are shown for p_1/p_0

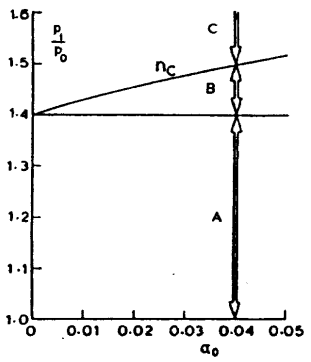

Fig.1 Characteristics of shock front in air-water mixture: A shock front with precursor B shock front with oscillatory shock front, C shock front without oscillatory shock front.

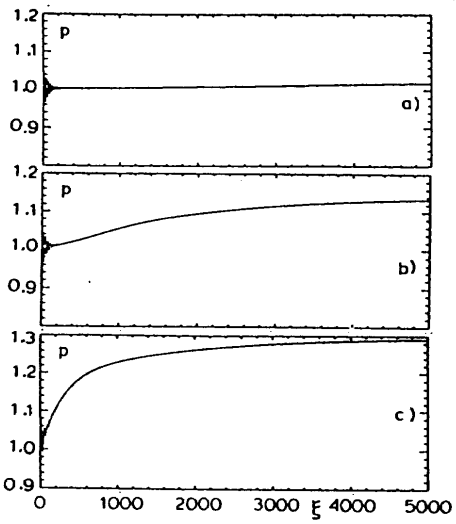

Fig.2 Pressure distributions in air-water mixture for $\alpha_0 = 0.05$: a) $p_1/p_0 = 1.05$, b) $p_1/p_0 = 1.15$, c) $p_1/p_0 = 1.30$.

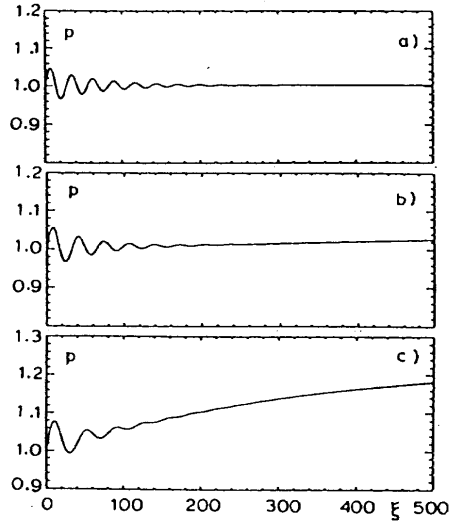

Fig.3 Precursors in air-water mixture.

=1.05, 1.15 and 1.3, respectively. Obviously the precursor becomes longer as the shock becomes weaker. The main shock, on the contrary, becomes more oscillatory with increasing shock strength. It is important to point out that the precursor obtained numerically is never the numerical noise but has a systematic structure. To show this, time enlarged pressure profiles are shown in Fig.3.

In Fig.4, a translational velocity profile for p_1/p_0=1.15 is shown, where the velocity slip is appreciable in all flow field.To investigate the effect of the velocity slip, the corresponding shocks for the mixture model are calculated by replacing Eq.(18) by $u_g=u_l$ or

$$\alpha = \frac{\alpha_0}{(1-\alpha_0)\rho_g+\alpha_0} . \qquad (24)$$

The results are shown in Fig.5 for p_1/p_0=1.05, 1.15 and 1.30. Obviously, the difference between the shocks in Figs.2 and 5 is remarkable.

As was discussed previously, one of the interesting approximations is the constant exponent model. In Fig.6, pressure profiles are shown for p_1/p_0=1.15 for the constant exponent model (n=1.0), where the damping coefficients Ψ evaluated following Devin is 114.4. The result is compared with that for the full model in this figure. Near the shock front,the constant exponent model yields relatively very sharp increase in pressure, which means the effect of the thermal damping will be underestimated near the shock front in this model.

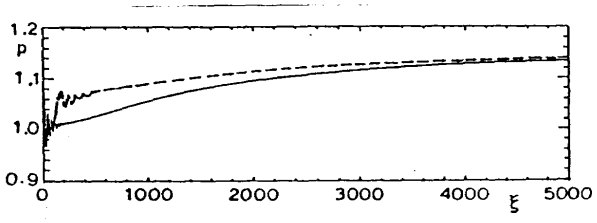

Fig.6 Comparison between the full model solution and the constant exponent- model solution for air-water mixture for p_1/p_0=1.15, α_0 = 0.05: ——— full model, — — — constant exponent model.

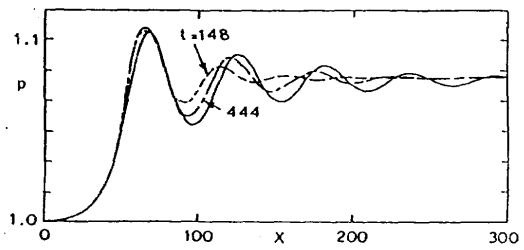

Fig.7 Time-convergency of shock front for mixture model with a constant exponent n=1 for p_2/p_0=1.2; - - - - - unsteady shock at t=148, — — — unsteady shock at t = 444, ———— stationary shock for p_1/p_0 = 1.0933.

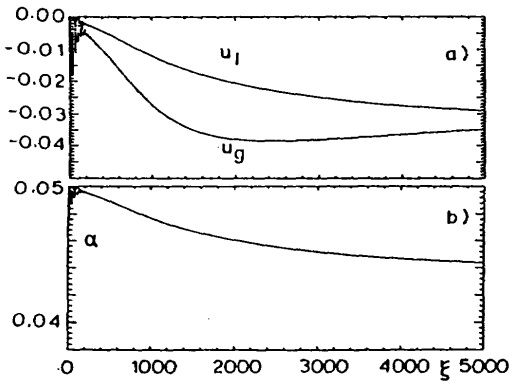

Fig.4 Distributions of bubble velocity u_g, liquid velocity u_l and void fraction α in air-water mixture for p_1/p_0 = 1.15, α_0 = 0.05.

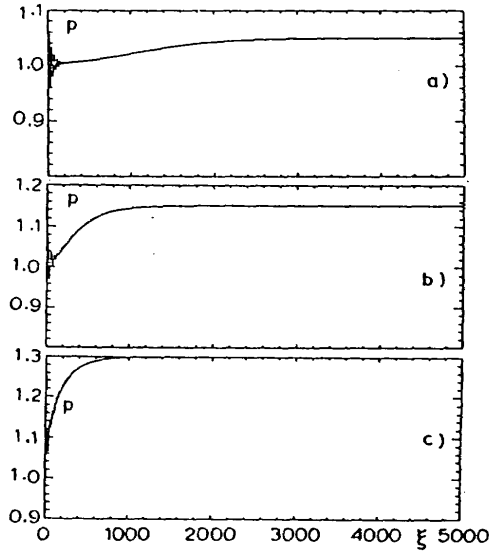

Fig.5 Pressure distributions in air-water mixture for the mixture model ($u_g = u_l$) for α_0= 0.05: a) p_1/p_0 = 1.05, b) p_1/p_0= 1.15, c) p_1/p_0 = 1.30.

IV. UNSTEADY SHOCK WAVES

A. Numerical scheme

Next we consider a shock tube problem, where the undisturbed conditions in the two chambers are uniform. Mathematically, hyperbolicity or well-posedness of the system is of crucial importance. Fortunately, the governing equations (1-4),(10) and (14) in conjunction with Eqs. (5-8),(18-19) constitute a well-posed system as an initial value problem, if the coefficient of diffusion force D_M is chosen to be some small positive constant[5]. Here we apply an Total-Variation-Diminishing (TVD) scheme developed by Chakravarthy & Osher[10].

B. Solutions for constant exponent model

In the shock tube problem, the initial flow

conditions in the high and the low pressure chambers separated by a diaphragm are specified as follows;

$$u_l=u_g=0,\ \alpha=\alpha_0,\ \rho_g=1,\ p=p_g=\Gamma, \quad \text{for } x>0$$
$$u_l=u_g=0,\ \alpha=\alpha_2,\ \rho_g=\rho_{g2},\ p=p_g=p_2, \quad \text{for } x\leqq 0 \tag{25}$$

where the diaphragm is located at x=0 and the subscript 2 denotes the high pressure chamber. Since the initial states are assumed to be in thermal equilibrium and the initial temperature is uniform throughout the whole flow region, we can put

$$p_2 = \Gamma\rho_{g2}, \quad \alpha_2 = \alpha_0/\rho_{g2}. \tag{26}$$

All the numerical results shown later are for p_0=1 atm, α_0=0.05, R_0=0.5 mm, D_M=0.01 and H=0.001.

A numerical solution to the mixture model ($u_g=u_l=u$) with a constant polytropic exponent (n=1) was performed and the results are shown in Fig. 7, where the unsteady pressure profiles are are compared with a stationary shock for p_1/p_0=1.0933. We can see a good time-convergency of the unsteady shock to the corresponding stationary shock.

The steady and unsteady shocks were calculated with completely different numerical schemes. In spite of this, the good agreement between the stationary and unsteady shocks for large t suggests sufficient reliability and accuracy of the present numerical schemes.

C. Solutions for full model

For analytical convenience, the initial conditions are given as follows,

$$u_g=u_l=0,\ \alpha=0.05,\ \rho_g=1.0,\ p=p_g=\Gamma, \text{ for } x\leqq 0,$$
$$u_g=u_l=-0.04,\ \alpha=0.05,\ \rho_g=1.0,\ p=p_g=\Gamma, \text{ for } x>0. \tag{27}$$

In this case, two uniform flows collide at x=0 at t=0 and two shocks are produced near x=0 which propagate into both the right and the left directions.

In Fig.8, distributions of the mixture pressure, the void fraction and the velocities are shown at the time-step 2700 (t=176). Oscillatory behavior of the shock front almost disappear and any symptom of the precursor is not seen at least in this stage.

V. CONCLUSIONS

Weak shock waves in a bubbly liquid were treated numerically. The weak shock has always a precursor which is essentially oscillatory and is followed by a relatively much more smooth main shock. The shocks with a precursor has not yet been observed experimentally. In light of this,

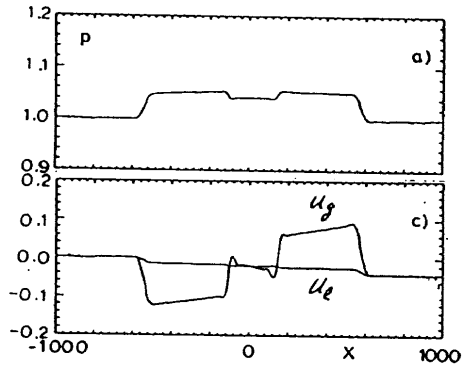

Fig.8 Distributions of mixture pressure and gas and liquid velocities at t=176.

the constant exponent model can be a good model at least for the analysis of weak shocks if the effect of the thermal dissipation is correctly taken into account, for example, in the correction factor Ψ.

Weak unsteady shocks for the full model were also treated. Neither instability nor the precursor was found. This might come from the fact that the undisturbed conditions are always fixed numerically.

References

1. I.J.Campbell and A.S.Pitcher, "Shock Waves in Liquid Containing Gas Bubbles," Proc.Royal. Soc.(London) A243, 534 (1958).
2. A. Crespo, "Sound and Shock Waves in Liquids Containing Bubbles," The Physics of Fluids 12, 2274 (1969).
3. L.Noordzij and L van Wijngaarden, "Relaxation effects, caused by relative motion, on shock waves in gas-bubble/liquid mixtures," J.Fluid Mech. 66, part. 1, 115 (1974).
4. A.E.Beylich and Ali Gülhan, "On the structure of nonlinear waves in liquid with gas bubbles," Phys. Fluids A 2, 1412 (1990).
5. R.Ishii, Y.Umeda, S.Murata and N.Shishido, "Bubbly flows through a converging-diverging nozzle," Physics of fluids A 5, 1630 (1993).
6. L. van Wijngaarden, "Hydrodynamic interaction between gas bubbles," J.Fluid Mech.77,27(1976)
7. G.K. Batchelor, "A new theory of a uniform fluidized bed," J.Fluid Mech.193,75 (1988).
8. C.Devin, J_R., "Survey of Thermal, Radiation, and Viscous Damping of Pulsating Air Bubbles in Water," J.Acoust.Soc.Amer.31, 1654 (1959).
9. A. Prosperetti, "The thermal behaviour of oscillating gas bubbles," J.Fluid Mech. 222, 587 (1991).
10. S.R.Chakravarthy, & S.Osher, "A new class of high accuracy TVD schemes for hyperbolic conservation laws," AIAA paper 85-0363(1985).